AIAA JOURNAL
Vol. 34, No. 11, November 1996

Nonlinear Analysis of Imperfect Metallic and Laminated Cylinders Under Bending Loads

Xiaozhi Huyan,* George J. Simitses,† and Ala Tabiei‡
University of Cincinnati, Cincinnati, Ohio 45221-0070

The nonlinear buckling of imperfect metallic and laminated cylindrical shells under axial compression, bending, and a combination of compression and bending is investigated. The effects of length-to-radius ratio, radius-to-thickness ratio, imperfection shape and amplitude, and boundary conditions on critical loads are considered. The finite element method is employed and the ANSYS computer code is selected to generate results. The effect of transverse shear deformation is included in the analysis. To acquire confidence in the solution methodology, results are produced and compared with those available by other solution techniques (analytical verification). Then, numerical results reflecting a wide range of length-to-radius ratios, radius-to-thickness ratios, and various imperfection shapes and amplitudes are presented and discussed. Among all conclusions, the most important one is that imperfection shapes substantially affect the critical loads. For each cylindrical configuration analyzed, certain imperfection shapes can be found, which make the cylinder extremely imperfection sensitive.

I. Introduction

THE primary consideration for designing and sizing jet engine casings is buckling under dynamic conditions. The loads that cause buckling are generated by the large forces resulting from rotor unbalance as a result of bladeout (loss of one or more blades during operation). These loads induce an end bending moment on the casing that is time dependent both in magnitude and direction. This bending moment is of finite but small duration. The time in which this moment reaches a peak value and vanishes is very short. The engine casing geometry can be approximated by a cylindrical shell. This configuration has numerous applications in real world structures. Airplane fuselages, submarine hulls storage bins, and missiles are but a few examples. Many times during service these systems are subjected to suddenly applied loads, such as blast loads on airplanes and submarine hulls and gust loads on storage bins and missiles. All of these situations can be simulated by cylindrical shells under dynamic bending moment or a combination of compressive and bending loads (Fig. 1).

For jet engine casings, the current practice is to estimate the peak moment, consider it as a static bending moment, and compare it with the static critical condition (buckling) of cylindrical shell under bending moment. This procedure has led to designs that are very conservative according to data from experimental verification studies. The weight penalty in most cases is in the 30–50% range. Moreover, since a large number of new casings are made of polymeric matrix composite materials and since the static analytical methods for these configurations are of questionable value, the weight penalty can exceed the 30–50% range.

Therefore, it is necessary to predict the static and dynamic critical loads of cylindrical shells under aforementioned loading conditions and to provide information that can be used in designs of cylindrical structures. In this paper, the static stability of metallic and laminated cylinders is studied and the following points are emphasized.

1) Cylindrical shells are subjected to axial compression, bending moment, or a combination of both loads.

2) Cylinders are geometrically imperfect. The effects of imperfect shapes and amplitudes on critical loads are discussed. Also, the effects of length-to-radius ratios, radius-to-thickness ratios, and boundary conditions are considered.

3) The transverse shear deformation is included in the analysis, and the reduced shear moduli are applied to avoid shear locking in the calculation for thin cylinders.

The results presented in this paper will serve as a baseline for comparison with those for dynamically loaded cylinders. The dynamic buckling analysis will be presented in the future.

II. Brief History

Numerous studies have been made on the stability of cylindrical shells with various construction materials. Imperfection sensitivity, load eccentricities, and material or constructional defects of cylindrical shells represent but a few subjects of these studies. See, for example, a review paper by Simitses.[1]

The study of cylindrical shells under bending moment is reviewed and described as follows. The earliest work on the shell buckling problem is attributed to Flügge.[2] He investigated the buckling of cylindrical shells under combined bending and compression and calculated the interaction curve for the radius-to-thickness ratio

$$12(R/t)^2 = 10^6$$

and for the longitudinal buckle half-wave-length-radius ratio

$$(m\pi R)/L = 1$$

For this case, he found that the ratio between the maximum critical stress for bending alone is 1.3 times the critical stress for pure compression. This calculation was then cited by Timoshenko[3] without the qualifying statement as to the assumed buckling wave length and has been used as a general rule since then. It was not until 1961 that more complete results were obtained by Seide and Weingarten.[4] They examined the case of an isotropic cylinder under pure bending. The results obtained by using the classical shell theory and the Galerkin procedure predicted that the maximum critical stress for bending is approximately equal to or slightly larger than the critical

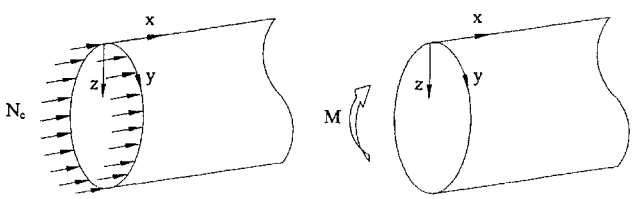

Fig. 1 Cylindrical shells under axial compression and pure bending moment.

Received Aug. 4, 1995; revision received March 20, 1996; accepted for publication June 10, 1996; also published in *AIAA Journal on Disc*, Volume 1, Number 4.

*Graduate Research Assistant, Department of Aerospace Engineering and Engineering Mechanics. Student Member AIAA.

†Professor, Department of Aerospace Engineering and Engineering Mechanics. Fellow AIAA.

‡Assistant Professor, Department of Aerospace Engineering and Engineering Mechanics. Member AIAA.

stress for axial compression. The edge effect is neglected in their solution. The maximum critical stress and the critical moment can be computed, respectively, as

$$(\sigma_{cr})_{max} = \frac{Et}{\sqrt{3(1-\mu^2)}R}$$

and

$$M_{cr} = \frac{\pi ERt^2}{\sqrt{3(1-\mu^2)}}$$

Bijlaard and Gallagher,[5] Johns,[6] and Libai and Durban[7,8] also considered the linear buckling problem of cylindrical shells subjected to nonuniform circumferentially axial loads or thermal loads.

The wide use of composite shells and the dramatic improvement in computer technology since the 1960s have generated considerable attention to the buckling problem. Ugural and Cheng[9] considered for the first time the buckling of laminated cylindrical shells under bending using Flügge's differential equations of equilibrium.[2] The results showed that the coupling between in-plane stretching and bending may have an important influence on the buckling loads of certain types of composite structures. Both Holston[10] and Mah et al.[11] employed Donnell theory and arrived at different conclusions for different loading conditions. The former predicted that the pure buckling bending stress is nearly equal to the uniform axial compression buckling stress, and the latter concluded that the critical bending stress is substantially higher than the compressive stress when the bending moment and axial compression are interacting with external pressure. Using Galerkin's method, Lou and Yaniv[12] investigated the same problem and solved both Donnell-type and Love-type equations. Numerical results reflecting a wide range of radius-to-thickness and length-to-radius ratios were presented and discussed. Linear stability analysis is employed in all of the preceding instances. Recently, Fuchs and Hyer[13,14] and Fuchs et al.[15] performed extensive studies on this topic. They induced bending by applying a known end rotation to each end of the cylinder, analogous to a beam in bending. A geometrically nonlinear special purpose analysis, based on Donnell theory, was developed to study the prebuckling response, and a finite element analysis was utilized to study the buckling and postbuckling responses of both perfect and imperfect cylindrical shells. In addition, experimental data were presented.

III. Methodology

The finite element method (FEM) is employed, and the ANSYS computer code is applied to analyze the problem in hand because of its extensive nonlinear solution and shell buckling capability and its ability to include general geometrical imperfection shapes. In addition, it is one of the suitable methods to predict dynamic critical loads of various cylinders in the future.

Owing to the significant discrepancy between theoretically predicted critical loads and the ones observed in experiments, it has been of great technical importance to clarify the effect of initial imperfections on the buckling of circular cylindrical shells. For this purpose, the midsurface of the cylinder under investigation is regarded as the reference surface and where given an initial imperfection. A cylindrical coordinate system is employed, and the nodal coordinate in the radial direction is taken as $r = R + w^0$, where R is the radius of the cylinder and w^0 is the amplitude of the imperfection shape.

Noor and Burton[16] and Simitses and Anastasiadis[17] have reported that shear deformation plays an important role in reducing the effective flexural stiffness of laminated plates and shells, especially in dynamic problems. For this reason, shell elements with eight nodes (shell 91 and shell 93)[18–20] are selected. There are six degrees of freedom at each node, three translations in the nodal x, y, and z directions, and three rotations about the nodal x, y, and z axes. Not only is the shear deformation included, but also the reduced shear moduli are used in the formation of stiffness matrices to avoid shear locking[18] for thin cylinders.

The axial compression and bending moment is transferred to nodal forces in the finite element analysis. Assuming that there are N_y elements and $2N_y$ nodes along the circumference, an axial

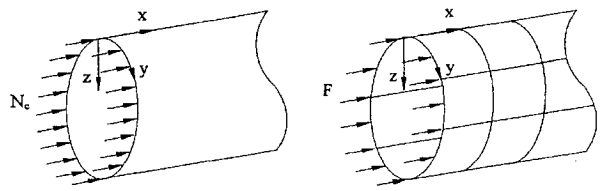

Fig. 2 Axial compression is converted to nodal forces.

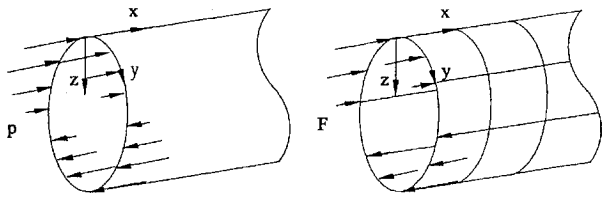

Fig. 3 Bending moment is converted to nodal forces.

compression N_c uniformly acting on the ends of the cylinder is converted by the following formula (see Fig. 2):

$$F(\theta) = \frac{2\pi RN_c}{2N_y} = \frac{\pi R}{N_y}N_c \tag{1}$$

For a cylinder under bending (Fig. 3), the bending moment M is first replaced by a distributed load

$$p = N_b \cos\theta \tag{2}$$

where N_b is the maximum load per unit circumference and

$$N_b = M/\pi R^2 \tag{3}$$

Then, the equivalent nodal forces of the bending moment can be calculated by

$$F(\theta) = \int_{\theta_1}^{\theta_2} pR\,d\theta = N_b R(\sin\theta_2 - \sin\theta_1) \tag{4}$$

where

$$\theta_1 = \theta - \Delta\theta \qquad \theta_2 = \theta + \Delta\theta$$
$$\Delta\theta = \frac{2\pi}{2\cdot 2N_y} = \frac{\pi}{2N_y} \tag{5}$$

When a cylinder is subjected to a combination of axial compression N_c and bending moment M, the nodal forces would be

$$F(\theta) = \int_{\theta_1}^{\theta_2} (N_c + p)R\,d\theta = \frac{\pi R}{N_y}N_c + \frac{M}{\pi R}(\sin\theta_2 - \sin\theta_1) \tag{6}$$

The nonlinear governing equations are solved with the aid of the Newton–Raphson procedure. The critical load is determined by gradually increasing the applied load to seek the limit point at which the solution does not converge.[21] It is important to recognize that an unconverged solution need not necessarily mean that the cylinder has reached its limit point. Therefore, the load-deflection history is tracked, and the cylinder modeling is refined if necessary to help in deciding the limit point. Moreover, a fine load increment is applied near the limit point, and the automatic load stepping and bisection functions[18] are turned on to obtain accurate results. The critical load obtained by the preceding methodology is almost the load at the limit point. In addition, an eigenvalue analysis is performed for perfect cylinders to obtain linear critical loads.

IV. Results and Discussion

A. Verification

Results for three different examples of simply supported cylinders under compressive and bending loads are generated to acquire confidence in the solution methodology. The material and geometrical properties, imperfection shapes, and all pertinent information are

Table 1 Critical loads of the laminated cylinder $[45/45/-45]_s$; units: 10^3 (N/m)/wave no.

$R/t = 30$	Compression						Bending	
$L/R = 1$	FOSD[21]	FOSD/SCF[21]	FEM (20 × 5)	FEM (30 × 10)	FEM (40 × 10)	%Diff.	(30 × 5)	N_b/N_c
$a = 0.01$	2258.9/2	2197.7/2	2210.0/2	2205.0/2	2205.0/2	0.36	2840.0	1.29
$a = 0.05$	2241.5/2	2180.2/2	2122.5/2	2130.0/2	2130.0/2	2.3	2872.5	1.35
$a = 0.10$	2215.2/2	2153.9/2	2032.5/2	2010.0/2	2010.0/2	−5	2745.5	1.37
Linear			2767.5				2867.7	1.04

Table 2 Critical loads of the laminated cylinder $[45/45/-45]_s$; units: 10^3 (N/m)/wave no.

$R/t = 60$	Compression			Bending	
$L/R = 1$	Ref. 21	FEM	% Diff.	load	N_b/N_c
$a = 0.01$	581.5/3	560/3	−3.6	655.0	1.17
$a = 0.05$	574.5/3	545/3	−5.1	637.5	1.17
$a = 0.10$	552.5/3	523/5	−5.3	610.0	1.12
Linear		760.2		792.6	1.04

Table 3 Critical loads of the laminated cylinder $[-45/45/-45]_s$; units: 10^3 (N/m)/wave no.

$R/t = 60$	Compression			Bending	
$L/R = 1$	Ref. 21	FEM	% Diff.	load	N_b/N_c
$a = 0.01$	613.0/2	636/2	3.75	682.5	1.07
$a = 0.05$	609.5/2	618/2	1.50	665.0	1.08
$a = 0.10$	599.0/2	598/2	0.00	640.0	1.07
Linear		842.7		935.8	1.11

Table 4 Critical loads of the laminated cylinder $[45/-45]_s$; units: (lb/in.)/wave no.

$R/t = 354$	Compression			Bending	
$L/R = 1$	Ref. 22	FEM	% Diff.	load	N_b/N_c
$a = 0.05$	——	127.0/9	——	135.0	1.07
$a = 0.10$	130.7/9	125.0/9	−4.20	132.9	1.06
$a = 0.50$	118.9/9	113.0/9	−5.10	122.4	1.09
$a = 1.00$	104.5/9	99.6.0/9	−4.70	105.8	1.06

Table 5 Critical loads of the laminated cylinder [90/60/30/0]; units: (lb/in.)/wave no.

$R/t = 354$	Compression			Bending	
$L/R = 1$	Ref. 22	FEM	% Diff.	load	N_b/N_c
$a = 0.50$	131.0/11	137.0/11	5.0	169.5	1.24
$a = 1.00$	86.8/11	89.3/11	−6.8	113.3	1.28
$a = 1.50$	——	52.5/11	——	71.8	1.39
$a = 2.00$	46.1/11	47.3/11	−3.1	61.5	1.10

taken from Refs. 21–23. The computed critical loads and the reference results are presented in Tables 1–7. For the first example (Tables 1–3), two six-layer symmetric laminated cylinders $[45/-45/-45]_s$ and $[-45/45/-45]_s$ with two radius-to-thickness ratios and axisymmetric type imperfection shapes are considered. The analytical results were reported in Ref. 21, and they corresponded to nonlinear kinematics and first-order shear deformation shell theory with or without a shear correction factor. The Galerkin procedure and the finite difference method were employed to solve the governing equations, and the critical loads were obtained through limit point instability.

The mesh sensitivity of the finite element method is established. It can be seen from Table 1 that the critical loads converge very well when 30 × 10 elements for a quarter of cylinder (30 elements in the circumferential direction and 10 elements in the longitudinal direction) are employed. Linear buckling loads are also presented in the last rows of the tables. The second example (Tables 4–6) consists of thin symmetric and unsymmetric four-layer boron/epoxy

Table 6 Critical loads of the laminated cylinder [0/30/60/90]; units: (lb/in.)/wave no.

$R/t = 354$	Compression			Bending	
$L/R = 1$	Ref. 22	FEM	% Diff.	load	N_b/N_c
$a = 0.50$	144.0/11	138.0/11	−4.0	154.5	1.12
$a = 1.00$	97.5/11	91.0/11	−6.8	113.3	1.12
$a = 1.50$	——	63.0/11	——	79.5	1.26
$a = 2.00$	48.0/11	49.0/8	−3.1	72.0	1.47

Table 7 Critical loads of the metallic cylindrical shell; units: (lb/in.)/wave no.

$R/t = 1000$	Compression			Bending	
$L/R = 1$	Ref. 23	FEM	% Diff.	load	N_b/N_c
$a = 0.00$	——	24.8/13	——	25.6/13	1.03
$a = 0.10$	22.7/13	23.8/13	4.80	25.4/13	1.07
$a = 1.00$	11.3/13	12.1/13	6.90	14.3/13	1.18
$a = 1.50$	——	8.5/13	——	9.8/13	1.16
$a = 2.00$	——	6.4/13	——	7.4/13	1.14

AVCO 5505 laminated cylinders with a radius-to-thickness ratio of 354. Transverse shear deformation is neglected in Ref. 22, and the imperfection shapes are symmetric type. An aluminum alloy cylindrical shell is also investigated in example 3, and results are presented in Table 7. The metallic cylinder is thin, and the radius-to-thickness value is as large as 1000.

Example 1. Thick Laminated Cylinders

Material: graphite/epoxy:

$$E_{11} = 149.617 \times 10^9 \text{ Pa} \qquad E_{22} = 9.928 \times 10^9 \text{ Pa}$$

$$E_{33} = 9.928 \times 10^9 \text{ Pa}$$

$$G_{12} = 4.481 \times 10^9 \text{ Pa} \qquad G_{13} = 4.481 \times 10^9 \text{ Pa}$$

$$G_{23} = 2.551 \times 10^9 \text{ Pa}$$

$$\mu_{12} = 0.28 \qquad \mu_{13} = 0.28 \qquad \mu_{23} = 0.45$$

Geometric properties:

$$R = 0.1905 \text{ m} \qquad L = 0.1905 \text{ m} \qquad t = 0.003175 \text{ m } (R/t = 60)$$

$$t = 0.00635 \text{ m } (R/t = 30)$$

Imperfection shape:

$$w^0_{(x,\theta)} = at[-\cos(2\pi x/L) + 0.1 \sin(\pi x/L) \cos n\theta] \qquad (7)$$

Example 2. Symmetric and Unsymmetric Laminated Cylinders

Material: boron/epoxy, AVCO 5505:

$$E_{11} = 30 \times 10^6 \text{ psi} \qquad E_{22} = 2.7 \times 10^6 \text{ psi}$$

$$E_{33} = 2.7 \times 10^6 \text{ psi}$$

$$G_{12} = 0.65 \times 10^6 \text{ psi} \qquad G_{13} = 0.65 \times 10^6 \text{ psi}$$

$$G_{23} = 0.37 \times 10^6 \text{ psi}$$

$$\mu_{12} = 0.21 \qquad \mu_{13} = 0.21 \qquad \mu_{23} = 0.45$$

Geometric properties:

$$R = 7.5\,\text{in.} \qquad L = 7.5\,\text{in.} \qquad h_{\text{ply}} = 0.0053\,\text{in.}$$

$$t = 4h_{\text{ply}} = 0.0212\,\text{in.} \qquad R/t = 354$$

Imperfection shape:

$$w^0_{(x,\theta)} = at \sin(\pi x/L)\cos n\theta \tag{8}$$

Example 3. Metallic Cylinder

Material: Aluminum alloy:

$$E = 10.5 \times 10^6\,\text{psi} \qquad \mu = 0.3$$

Geometric properties:

$$R = 4\,\text{in.} \qquad L = 4\,\text{in.} \qquad t = 0.004\,(R/t = 1000)$$

Imperfection shapes:

$$w^0_{(x,\theta)} = at[-\cos(2\pi x/L) + 0.1\,\sin(\pi x/L)\cos n\theta] \tag{9}$$

The present results are compared with those obtained previously from Refs. 21–23 for the case of uniform axial compression (see Tables 1–7). The differences are within 5% with only a few exceptions. Considering that the cylinder is sensitive to geometrical imperfection and hence also sensitive to the methodology, the preceding results are satisfactory. From generated results, the maximum critical bending stresses are found to be 6–30% higher than the critical axial compression stresses in most cases. This is in agreement with the conclusion obtained by former researchers. Therefore, the methodology utilized in this paper is suitable for analysis of cylindrical shells including isotropic and anisotropic, thin and thick, and symmetric and unsymmetric laminated shells under axial compression and bending loads.

The effects of several parameters on critical loads of metallic and laminated cylindrical shells are investigated hereafter. The radius is assumed to be 4 in., and the material properties are those of example 3 for metallic cylinders. For laminated cylinders, the material properties are the same as those of example 2. The thickness of each layer is taken as 0.0053 in., and the thickness of a laminated cylinder depends on the number of layers. All cylinders are simply supported except those in Sec. IV.D.

B. Effect of Length-to-Radius and Radius-to-Thickness Ratios on Critical Loads

Tables 8 and 9 present critical loads of metallic cylinders under compressive and bending loads, respectively. Five length-to-radius (L/R) ratios and five radius-to-thickness (R/t) ratios are considered. For axially compressed cylinders, the critical loads seem to be independent of L/R values and are approximately proportional to $(R/t)^2$. For thick and moderately thick cylinders under bending, the critical loads decrease with increasing L/R values. The thicker the cylinder, the more the critical load decreases. For instance, when the cylinders extend from $L/R = 1$ to 5, the critical loads reduce 25% for $R/t = 25$ and 14% for $R/t = 50$.

Table 8 Critical loads of metallic cylinders under compression; units: lb/in.

	R/t					
L/R	25	50	100	200	500	1000
1	38,250	9871	2400	610.8	97.88	24.68
2	37,861	9608	2450	604.9	98.40	24.35
3	37,413	9624	2402	607.1	98.39	24.35
4	37,700	9561	2402	607.1	98.39	24.35
5	37,638	9533	2402	605.6	98.73	24.35

Table 9 Critical loads of metallic cylinders under bending loads; units: lb/in.

	R/t					
L/R	25	50	100	200	500	1000
1	36,667	9237	2335	602.9	100.7	25.7
2	35,200	9133	2344	606.9	101.2	25.5
3	33,111	8970	2335	605.3	101.1	25.5
4	30,441	8611	2317	605.3	101.4	25.5
5	27,330	7981	2261	601.0	101.3	25.5

Table 10 Critical loads of laminated cylinders (R/t = 354) under compression; units: lb/in.

	L/R				
Layup	1	2	3	4	5
$[0/0]_s$	270.9	274.8	274.8	274.8	274.8
$[30/-30]_s$	168.3	169.1	166.7	166.7	166.7
$[45/-45]_s$	128.3	129.1	129.1	129.1	129.1
$[60/-60]_s$	166.8	169.1	169.1	169.1	168.1
$[90/90]_s$	315.7	312.3	312.3	312.3	312.3
$[0/90]_s$	359.2	357.8	356.8	356.8	356.8
$[90/0]_s$	364.7	365.7	365.7	365.7	365.7
[90/60/30/0]	133.6	133.6	133.6	131.1	133.1
[0/30/60/90]	169.1	166.7	164.7	164.7	164.7
[30/0/90/60]	197.8	200.2	200.2	199.8	200.2

Table 11 Critical loads of laminated cylinders (R/t = 354) under bending loads; units: lb/in.

	L/R				
Layup	1	2	3	4	5
$[0/0]_s$	293.5	294.6	292.6	281.2	257.0
$[30/-30]_s$	183.5	184.4	184.4	182.4	182.4
$[45/-45]_s$	143.5	142.4	142.4	142.4	142.4
$[60/-06]_s$	181.7	182.4	184.4	182.4	182.4
$[90/90]_s$	337.9	332.6	332.6	332.6	332.6
$[0/90]_s$	381.4	381.4	381.4	381.4	381.4
$[90/0]_s$	381.4	381.4	381.4	381.4	381.4
[90/60/30/0]	211.1	209.1	206.7	206.7	206.7
[0/30/60/90]	184.4	182.4	182.4	182.4	182.4
[30/0/90/60]	206.7	206.7	206.7	206.7	206.7

The critical compression and bending loads of laminated cylinders are described in Tables 10 and 11, respectively. Unidirectional, angle-ply, cross-ply, and unsymmetric stacking sequences are considered. The critical loads of laminated cylinders under compression, as in the case of metallic cylinders, are independent of length-to-radius ratios. Moreover, the critical loads of laminated cylinders of $R/t = 354$ under bending vary little with L/R except for the unidirectional laminated cylinder $[0/0]_s$. In this case, critical loads decrease 13% from $L/R = 1$ to 5.

C. Effects of Imperfection Shapes and Magnitudes on Critical Loads

The imperfection substantially influences the critical loads of cylindrical shells. Consider, for instance, the metallic cylinder with $L/R = 3$ and $R/t = 500$ and the imperfection shape

$$w^0_{(x,\theta)} = at\cos(n\theta)\cos\left\{m\pi\left[(x/L) - \tfrac{1}{2}\right]\right\} \tag{10}$$

Critical compression loads are computed by using different values of m and n. A few results are presented in Table 12 for $a = 2$. The imperfection shape with $m = 9$ and $n = 6$ yields the lowest critical load. This imperfection shape is close to the linear buckling mode of the cylinder. Table 13 lists the critical loads of the metallic cylinder with that imperfection shape of both positive and negative amplitudes. It is found that both signs lead to the same critical compression loads. For cylinders subjected to bending moment, they lead to different bending critical loads. The small outward imperfection shape (negative a) produces stabilizing effects.

Following Koiter's suggestion,[24] the linear buckling mode is employed as the imperfection shape because it yields the lowest critical load (limit point). The preceding results support this contention. Thus, the buckling mode of a cylinder under axial compression is first obtained through a linear buckling analysis. Then, this mode is applied as the imperfection shape with various amplitudes, and the limit point of the cylinder is calculated. In addition, the same imperfection shape is employed in the bending case to compare the critical compression load and critical bending load. Tables 14–18

Table 12 Critical loads of the metallic cylinder with various imperfection shape (L/R = 3, R/t = 500 and a = 2); units: lb/in.

m	n	$(N_c)_{cr}$
1	2	96.62
1	5	78.78
1	6	56.28
1	8	69.06
2	6	39.72
3	6	48.28
4	6	25.73
9	8	20.84
9	6	16.50
Perfect (a = 0)		98.39

Table 13 Critical loads of the metallic cylinder with various imperfection amplitude values (L/R = 3 and R/t = 500); units: lb/in.

	Compression		Bending	
a	$+a$	$-a$	$+a$	$-a$
0.00	98.39	98.39	101.4	101.4
0.10	94.74	94.74	99.61	101.5
0.25	88.06	88.06	94.05	96.67
0.50	62.39	62.39	69.85	65.73
0.75	43.39	43.39	48.28	45.10
1.00	31.84	31.84	36.73	33.83
1.50	19.62	19.62	26.27	23.65
2.00	16.50	16.50	22.61	21.73

Table 14 Critical loads of the laminated cylinder $[0/0]_s$; units: lb/in.

	L/R					
	1 (m = 7, n = 4)		2 (m = 15, n = 4)		5 (m = 35, n = 4)	
a	Comp.	Bending	Comp.	Bending	Comp.	Bending
0.00	270.9	293.5	274.8	294.6	274.8	257.0
0.01	135.6	160.2	135.6	155.8	133.1	146.9
0.025	131.1	142.4	131.1	140.0	131.1	135.6
0.05	129.1	138.0	126.7	135.6	126.7	131.1
0.075	126.7	133.6	124.7	133.1	124.7	126.7
0.10	124.7	131.1	122.2	129.1	124.7	124.7
0.25	117.8	126.7	115.8	122.2	120.2	117.8
0.50	111.3	119.8	111.3	117.8	120.2	113.3

present results of five laminated cylinders ($R/t = 354$). In all cases, the imperfection shape is given by

$$w^0_{(x,\theta)} = \begin{cases} at\,(2x/L)\cos(n\theta)\cos\left\{m\pi\left[\frac{1}{2} - (x/L)\right]\right\} & x \le L/2 \\ at\,[2 - (2x/L)]\cos(n\theta)\cos\left[m\pi\left[(x/L) - \frac{1}{2}\right]\right]\} & x \ge L/2 \end{cases} \tag{11}$$

except for cylinder $[45/-45]_s$. Although the perfect orthotropic cylinders $[0/0]_s$ and $[90/90]_s$ and the cross-ply cylinder $[0/90]_s$ yield the stronger configurations (higher critical loads), they are more sensitive to initial geometric imperfections than the other laminated cylinders $[30/-30]_s$ and $[45/-45]_s$. The critical loads drop significantly for imperfection amplitude from $a = 0$ to 0.01. On the other hand, the laminated cylinders $[30/-30]_s$ and $[45/-45]_s$ do not behave in the same manner, and their critical loads reduce gradually with increasing imperfection amplitude.

D. Effect of Boundary Conditions

One geometrically imperfect metallic cylinder and eight geometrically perfect laminated cylinders are employed to investigate the effect of boundary conditions. Figure 4 presents the results of the

Table 15 Critical loads of the laminated cylinder $[30/-30]_s$; units: lb/in.

	L/R					
	1 (m = 7, n = 4)		2 (m = 15, n = 4)		5 (m = 35, n = 4)	
a	Comp.	Bending	Comp.	Bending	Comp.	Bending
0.00	169.1	184.4	169.1	184.4	168.1	182.4
0.01	169.1	184.4	169.1	184.4	166.7	182.4
0.025	169.1	184.4	169.1	184.4	166.7	182.4
0.05	169.1	184.4	169.1	184.4	166.7	182.4
0.075	169.1	184.4	169.1	182.4	166.7	180.0
0.10	166.7	182.4	169.1	180.0	166.7	171.1
0.25	138.0	148.9	129.1	126.7	129.1	122.2
0.50	91.11	95.56	80.22	80.22	79.77	77.78

Table 16 Critical loads of the cylinder $[45/-45]_s$ with $w^0_{(x,\theta)} = at\cos(n\theta)\cos\{m\pi[(x/L) - \frac{1}{2}]\}$; units: lb/in.

	L/R					
	1 (m = 7, n = 4)		2 (m = 17, n = 4)		5 (m = 39, n = 4)	
a	Comp.	Bending	Comp.	Bending	Comp.	Bending
0.00	129.1	143.5	129.1	142.4	129.1	142.4
0.01	126.7	140.0	129.1	142.4	129.1	142.4
0.025	124.7	137.6	127.1	140.0	128.7	135.6
0.05	120.2	131.1	124.7	131.1	124.7	124.7
0.075	113.3	126.7	115.8	122.2	117.8	117.8
0.10	108.9	120.2	110.9	115.8	111.3	110.9
0.25	82.22	95.56	89.11	91.11	86.67	86.67
0.50	60.00	73.33	74.89	80.22	68.88	75.78

Table 17 Critical loads of the laminated cylinder $[90/90]_s$; units: lb/in.

	L/R					
	1 (m = 3, n = 14)		2 (m = 5, n = 14)		5 (m = 11, n = 14)	
a	Comp.	Bending	Comp.	Bending	Comp.	Bending
0.00	315.7	337.9	312.3	332.6	312.3	332.6
0.01	153.3	169.1	144.4	169.1	151.3	177.0
0.025	131.1	146.9	124.2	144.4	129.1	155.8
0.05	117.8	129.1	115.8	126.7	117.8	135.6
0.075	113.3	122.2	108.9	119.8	113.3	124.7
0.10	108.9	115.8	104.4	113.3	108.9	119.8
0.25	89.11	95.56	86.67	91.11	93.55	98.00
0.50	77.78	80.22	73.33	73.33	84.67	86.67

Table 18 Critical loads of the laminated cylinder $[0/90]_s$; units: lb/in.

	L/R					
	1 (m = 5, n = 13)		2 (m = 11, n = 13)		5 (m = 27, n = 13)	
a	Comp.	Bending	Comp.	Bending	Comp.	Bending
0.00	359.2	381.4	357.8	381.4	356.8	381.4
0.01	180.0	204.7	169.1	195.8	157.8	182.4
0.025	155.8	180.0	151.3	166.7	154.3	162.2
0.05	148.9	162.2	151.3	160.2	151.3	157.8
0.075	146.9	157.8	148.9	157.8	148.9	153.3
0.10	144.4	153.3	146.9	153.3	146.9	150.9
0.25	133.6	138.0	135.6	138.0	135.6	135.6
0.50	122.2	124.7	124.7	124.7	122.2	122.2

metallic cylinder with $L/R = 3$, $R/t = 500$, $R = 4$ in., and the imperfection shape

$$w^0_{(x,\theta)} = at\cos(6y)\cos\left\{9\pi\left[(x/L) - \frac{1}{2}\right]\right\} \tag{12}$$

For $a < 0.5$, the critical loads for clamped cylinders are about 10% higher than those for simply supported cylinders under compression and bending, respectively. The differences diminish when $a \ge 0.5$. Table 19 presents critical loads of laminated cylinders under compression and bending loads for both simply supported and clamped boundary conditions. The values of $L/R = 5$, $R/t = 235$, and $R = 7.5$ in. are taken as the geometric parameters of the laminated cylinders. For cylinders under compression, the critical compression loads of clamped cylinders are approximately

Table 19 Critical loads of laminated cylinders for simply supported (SS) and clamped boundary conditions with $L/R = 5$, $R/t = 236$, and $a = 0$; units: lb/in.

	Cases			
	Compression		Bending	
Layup	SS	Clamped	SS	Clamped
$[0/45/-45]_s$	502.22	546.67	520.00	560.44
$[45/-45/0]_s$	606.89	695.78	622.67	626.67
$[30/45/-45]_s$	326.44	351.11	338.22	347.11
$[45/-45/30]_s$	382.67	393.56	368.88	368.89
$[90/45/-45]_s$	651.33	745.11	727.33	803.11
$[45/-45/90]_s$	498.22	537.78	520.00	564.44
$[90/0/90]_s$	957.67	1064.3	957.67	957.60
$[0/90/0]_s$	957.67	1033.7	930.00	931.00

10–15% higher than those of simply supported cylinders. The critical bending loads are a little less sensitive to the boundary conditions, and the largest difference observed is 10%.

E. Cylinders Under Combined Loads

Critical loads of metallic and laminated cylinders under combined compressive and bending loads are shown in Figs. 5 and 6, respectively. These loads are exerted on the ends of cylinders simultaneously. The imperfection shape

$$w^0_{(x,\theta)} = at\cos(2\theta)\cos\left\{14\pi\left[(x/L) - \tfrac{1}{2}\right]\right\} \tag{13}$$

is employed for metallic cylinder with the following geometry, $L/R = 2$, $R/t = 1000$, and $R = 4.0$ in., and

$$w^0_{(x,\theta)} = at\cos(4\theta)\cos\left\{7\pi\left[(x/L) - \tfrac{1}{2}\right]\right\} \tag{14}$$

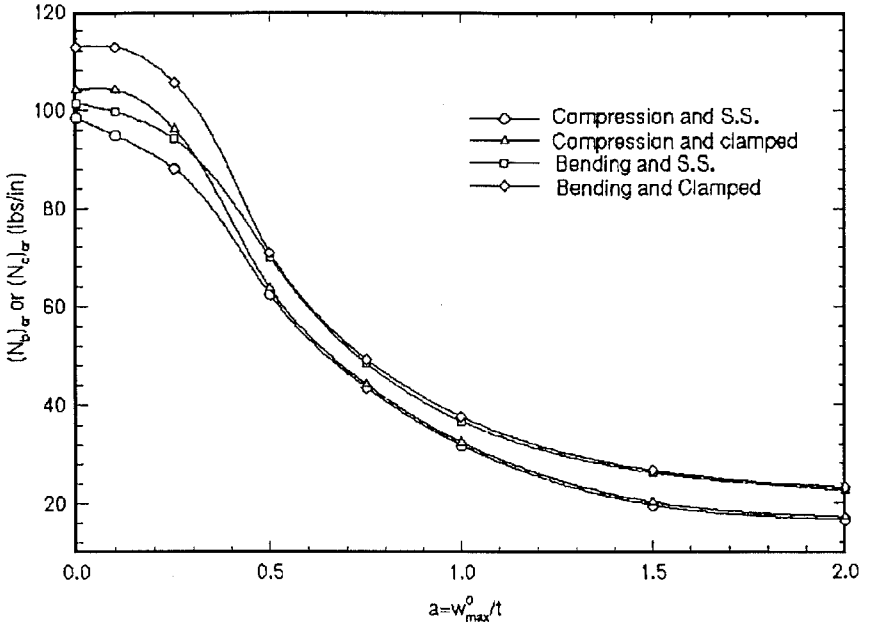

Fig. 4 Critical loads of simply supported and clamped metallic cylinders.

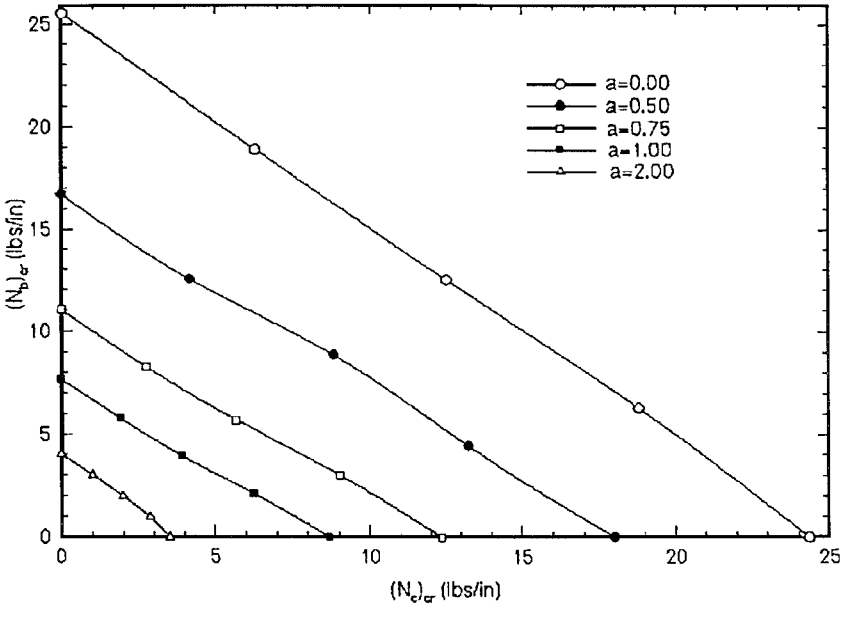

Fig. 5 Critical loads of the metallic cylinder under combined compressive and bending loads.

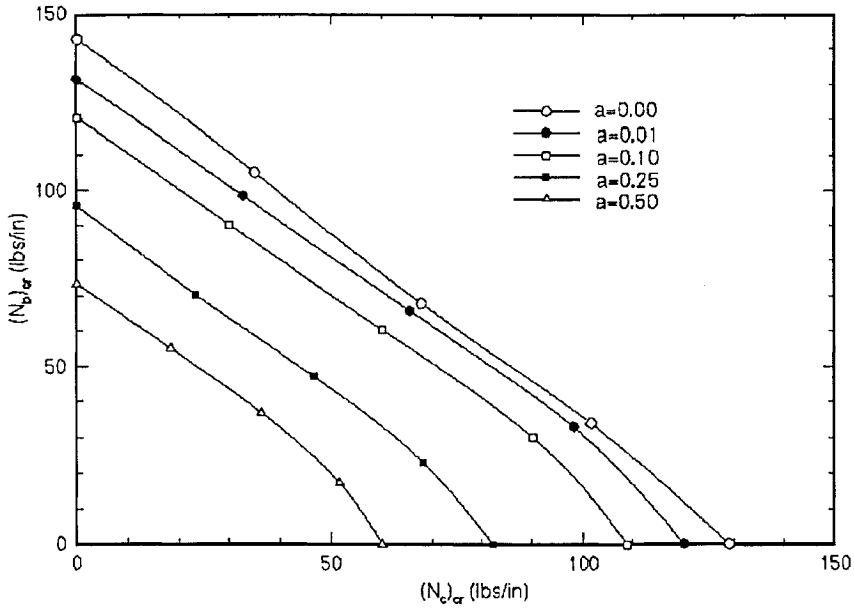

Fig. 6 Critical loads of the laminated cylinder $[45/-45]_s$ under combined loads.

is employed for the laminated cylinder $[45/-45]_s$ with $L/R = 1$, $R/t = 354$, and $R = 7.5$ in. It can be observed that the relationship between critical loads of cylinders under compression and bending is almost linear except those of the laminated cylinder under very high compression load.

V. Conclusion

The following can be listed as the most noteworthy conclusions of the investigation.

1) The methodology is reliable and suitable for all configurations. In addition, it is easy to apply.

2) The critical loads of thick metallic cylinders and laminated cylinders with certain stacking sequences under bending decrease with increasing L/R values. In all other cases, the critical loads are independent of the length-to-radius ratio.

3) The imperfection shapes have significant effect on critical loads. For every configuration (metallic or laminated, thick or thin, long or short, under compression or bending, simply supported or clamped), the worst shape is the one corresponding to the linear buckling mode.

4) Boundary conditions affect the critical loads of perfect cylinders and imperfect cylinders with small imperfection amplitudes ($a < 0.5$). For larger amplitudes, the differences of critical loads between simply supported and clamped boundary conditions are negligibly small.

5) The critical loads of orthotropic laminated cylinders are larger than those of angle-ply laminated cylinders, but the orthotropic cylinders are more sensitive to initial geometric imperfections than the angle-ply laminated cylinders. This is true for both compressive and bending load cases.

Acknowledgments

This work is supported by the Ohio Aerospace Institute under its Core Research Program. Its financial support is gratefully acknowledged. Moreover, in-kind support is provided by GE Aircraft Engines. In addition, the support provided by the Ohio Supercomputer Center in terms of time on the Cray under Grant PES443-5 is appreciated. The authors extend their thanks to Steve Mitchell and Mike Braley.

References

[1]Simitses, G. J., "Buckling and Postbuckling of Imperfect Cylindrical Shells, A Review," *Applied Mechanics Reviews*, Vol. 39, No. 10, 1986, pp. 1517–1524.

[2]Flügge, W., "Die Stabilität der Kreiszylinderschale," *Ingenieur-Archiv*, III. Band, 5, Heft, 1932, pp. 486–491, 501–506.

[3]Timoshenko, S. P., *Theory of Elastic Stability*, McGraw–Hill, New York, 1932.

[4]Seide, P., and Weingarten, V. I., "On the Buckling of Circular Cylindrical Shells Under Pure Bending," *Journal of Applied Mechanics*, Vol. 28, No. 3, 1961, pp. 112–116.

[5]Bijlaard, P. P., and Gallagher, R. H., "Elastic Instability of a Cylindrical Shell Under Arbitrary Circumfererntial Variation of Axial Stress," *Journal of the Aerospace Sciences*, Vol. 27, No. 11, 1960, pp. 854–859.

[6]Johns, D. J., "On the Linear Buckling of Circular Cylindrical Shells Under Asymmetric Axial Compressive Stress Distribution," *Journal of the Royal Aeronautical Society*, Dec. 1996, pp. 1095–1097.

[7]Libai, A., and Durban, D., "A Method for Approximate Stability Analysis and Its Application to Circular Cylindrical Shells Under Circumferentially Varying Loads," *Journal of Applied Mechanics*, Vol. 40, No. 4, 1973, pp. 971–976.

[8]Libai, A., and Durban, D., "Buckling of Cylindrical Shells Subjected to Non-Uniform Axial Loads," *Journal of Applied Mechanics*, Vol. 44, No. 4, 1977, pp. 714–719.

[9]Ugural, A. G., and Cheng, S., "Buckling of Composite Cylindrical Shells Under Pure Bending," *AIAA Journal*, Vol. 6, No. 2, 1968, pp. 349–354.

[10]Holston, A., Jr., "Buckling of Inhomogeneous Anisotropic Cylindrical Shells by Bending," *AIAA Journal*, Vol. 6, No. 10, 1968, pp. 1837–1841.

[11]Mah, G. B., Almroth, B. O., and Pittner, E. V., "Buckling of Orthotropic Cylinders," *AIAA Journal*, Vol. 6, No. 4, 1968, pp. 598–602.

[12]Lou, K. A., and Yaniv, G., "Buckling of Circular Cylindrical Composite Shells Under Axial Compression and Bending Loads," *Journal of Composite Materials*, Vol. 25, No. 2, 1991, pp. 162–187.

[13]Fuchs, H. P., and Hyer, M. W., "The Bending Responses of Thin-Walled Laminated Composite Cylinders," *Composite Structures*, Vol. 22, 1992, pp. 87–107.

[14]Fuchs, H. P., and Hyer, M. W., "The Nonlinear Bending Responses of Thin-Walled Laminated Composite Cylinder," *Proceedings of the AIAA 33rd Structures, Structural Dynamics, and Materials Conference* (Dallas, TX), AIAA, Washington, DC, 1992, pp. 70–78 (AIAA Paper 92-2230).

[15]Fuchs, H. P., Hyer, M. W., and Starnes, J. H., Jr., "Numerical and Experimental Investigation of the Bending Responses of Thin-Walled Composite Cylinders," Center for Composite Materials and Structures, Virginia Polytechnic Inst. and State Univ., CCMS-93-19, VPI-E-93-11, Blacksburg, VA, Sept. 1993.

[16]Noor, A. K., and Burton, W. S., "Assessment of Computational Models for Multilayered Composite Shells," *Applied Mechanics Reviews*, Vol. 43, No. 4, 1990, pp. 67–96.

[17]Simitses, G. J., and Anastasiadis, J. S., "Shear Deformation Theories for Cylindrical Laminates—Equilibrium and Buckling with Application," *AIAA Journal*, Vol. 30, No. 3, 1992, pp. 826–834.

[18]Anon., "ANSYS User's Manual for Revision 5.0," Swanson Analysis System, Inc., Dec. 1992

[19]Ahmad, S., Irons, B. M., and Zienkiewicz, O. C., "Analysis of Thick and Thin Shell Structures by Curved Finite Element," *International Journal for Numerical Methods in Engineering*, Vol. 2, 1970, pp. 419–451.

[20]Cook, R. D., Malkus, D. S., and Plesha, M. E., *Concepts and Applications of Finite Element Analysis*, Wiley, New York, 1989.

[21]Tabiei, A., "Buckling Analysis of Moderately Thick Laminated Shells," Ph.D. Dissertation, Dept. of Aerospace Engineering and Engineering Mechanics, Univ. of Cincinnati, OH, May 1994.

[22]Simitses, G. J., Shaw, D., and Sheinman, I., "Imperfection Sensitivity of Laminated Cylindrical Shells in Torsion and Axial Compression," *Composite Structures*, Vol. 4, 1985, pp. 335–360.

[23]Simitses, G. J., Shaw, D., Sheinman, I., and Giri, J., "Imperfection Sensitivity of Fiber-Reinforced Composite Thin Cylinders," *Composites Science and Technology*, Vol. 22, 1985, pp. 257–276.

[24]Koiter, W. T., "General Equation of Elastic Stability of Thin Cylinder," *Proceedings of the 70th Anniversary Symposium on the Theory of Shells to Honor L. H. Donnell*, edited by D. Muster, Univ. of Houston, TX, 1967.